

THE DISCOVERY OUTBURST OF THE X-RAY TRANSIENT IGR J17497–2821 OBSERVED
WITH *RXTE* AND ATCA

JÉRÔME RODRIGUEZ¹, MARION CADOLLE BEL^{2,1}, JOHN A. TOMSICK^{3,4}, STÉPHANE CORBEL¹,
CATHERINE BROCKSOPP⁵, ADA PAIZIS⁶, SIMON E. SHAW^{7,8}, ARASH BODAGHEE^{8,9}

Accepted in ApJ Letters

ABSTRACT

We report the results of a series of *RXTE* and ATCA observations of the recently-discovered X-ray transient IGR J17497–2821. Our 3–200 keV PCA+HEXTE spectral analysis shows very little variations over a period of ~ 10 days around the maximum of the outburst. IGR J17497–2821 is found in a typical Low Hard State (LHS) of X-ray binaries (XRB), well represented by an absorbed Comptonized spectrum with an iron edge at about 7 keV. The high value of the absorption ($\sim 4 \times 10^{22} \text{ cm}^{-2}$) suggests that the source is located at a large distance, either close to the Galactic center or beyond. The timing analysis shows no particular features, while the shape of the power density spectra is also typical of LHS of XRBs, with $\sim 36\%$ RMS variability. No radio counterpart is found down to a limit of 0.21 mJy at 4.80 GHz and 8.64 GHz. Although the position of IGR J17497–2821 in the radio to X-ray flux diagram is well below the correlation usually observed in the LHS of black holes, the comparison of its X-ray properties with those of other sources leads us to suggest that it is a black hole candidate.

Subject headings: accretion — black hole physics — stars: individual (IGR J17497–2821, Cyg X-1, XTE J1550–564, Swift J1753.5–0127)

1. INTRODUCTION

Transient X-ray Binaries (XRB) are known to show a series of different X-ray spectral states during their outbursts. A certain number of these objects have, however, undergone outbursts during which they remained in the Low Hard State (LHS) (e.g. Hynes et al. 2000; Brocksopp et al. 2004; Rodriguez et al. 2006a; Cadolle Bel et al. 2006a). A strong correlation exists between the radio and X-ray fluxes during this state (Corbel et al. 2003; Gallo et al. 2003). This may indicate some influence of the radio jet in the X-ray domain. The study of the LHS should, therefore, reveal important clues to the connection between the accretion and ejection processes. Interestingly, black hole (BH) transients are more radio loud than neutron stars (NS) by a factor of ~ 30 (Migliari & Fender 2006) in the LHS.

IGR J17497–2821 was discovered with ISGRI on-board *INTEGRAL* on Sept. 17, 2006 as a new hard XRB (Soldi et al. 2006) at Galactic coordinates $l=0.97^\circ$, $b=-0.46^\circ$. Given that the line of sight to the source passes close to the Galactic Center, and assuming a distance of 8 kpc, Kuulkers et al. (2006) estimated a 2–100 keV (unabsorbed) luminosity of $\sim 10^{37} \text{ erg/s}$. The position and luminosity strongly indicate IGR J17497–2821 is a Galactic XRB. The preliminary spectral analysis of their *INTEGRAL* data led Kuulkers et al. (2006) to further

suggest the source was in a LHS typical of BH and NS XRBs. A follow up observation with the Chandra X-ray Observatory allowed a fine X-ray position to be given at $\alpha = 17^h 49^m 38.037^s$, $\delta = -28^\circ 21' 17.37''$ ($\pm 0.6''$, at 90% confidence, Paizis et al. 2006). This refined X-ray position permitted Paizis et al. (2006) to identify the probable optical/IR counterpart, and classify it as a red giant K-type star making IGR J17497–2821 a Low Mass X-ray Binary (LMXB).

Soon after the discovery, we triggered our *RXTE* program P92016 as well as radio observations with the Australian Telescope Compact Array (ATCA), aiming to identify the nature of the system. We report here the results of those campaigns.

2. OBSERVATIONS AND DATA ANALYSIS

2.1. *X-ray observations*

Our *RXTE* program has been divided into seven pointings, the details of which are reported in Table 1. Fig. 1 shows the 3–30 keV *RXTE*/PCA and 15–50 keV Swift/BAT light curves of IGR J17497–2821 over the outburst. The PCA data were reduced in the same way as in Rodriguez et al. (2003), although with the latest version of the HEASOFT software package. Since the source is located in a crowded area, standard background subtraction is not sufficient to remove the contribution of other sources and

¹AIM Astrophysique Interaction Multi-échelles CEA Saclay, DSM/DAPNIA/SAP, F-91191 Gif sur Yvette, Cedex France

²European Space Astronomy Centre, Villafranca del Castillo, 28629 Madrid Spain

³Space Sciences Laboratory, 7 Gauss Way, University of California, Berkeley, CA 94720, USA

⁴Center for Astrophysics and Space Sciences, 9500 Gilman Drive, Code 0424, University of California at San Diego, La Jolla, CA 92093, USA

⁵Mullard Space Science Laboratory, University College London, Holmbury St. Mary, Dorking, Surrey RH5 6NT, UK

⁶IASF Milano–INAF, Via Bassini 15, 20133 Milano, Italy

⁷School of Physics and Astronomy, University of Southampton, SO17 1BJ, UK

⁸INTEGRAL Science Data Centre, Chemin d’Ecogia, 16, 1290 Versoix, Switzerland

⁹Observatoire Astronomique de l’Université de Genève, Chemin des Maillettes 51, CH-1290 Sauverny, Switzerland

the Galactic Bulge (about 10 mCrab between 2-10 keV, Markwardt & Swank (2006)). In order to better estimate the sky background at the source position, we analyzed an *RXTE* observation of the nearby BH Candidate XTE J1748-288 made at the end of its 1998 outburst, when the source flux was comparable with that of the Galactic background (Obs. Id 30185-01-20-00). The best fitted model of this observation was then used as an extra background component for the spectral fittings of all our observations.

For HEXTE, we extracted spectral data from the Cluster B unit only, since Cluster A no longer obtains a background measurement because the rocking has ceased. We checked that “plus” and “minus” offset pointings gave similar spectra (indicating that no active sources contributed to the background) and combined the two pointings to obtain background spectra. The remaining processes for HEXTE reduction are similar to the procedures presented in Rodriguez et al. (2003). The PCA and HEXTE spectra of each observation were fitted simultaneously in XSPEC v11.3.2t between 3 and 200 keV. A normalization constant was introduced to account for calibration uncertainties between PCA and the single HEXTE cluster.

High resolution light curves were extracted from Good Xenon and Event data with a time resolution of $\sim 122\mu\text{s}$ allowing us to study the temporal properties of the source up to 4096 Hz. In order to restrict the background effects at low and high energies, we restricted the extraction to the $\sim 5\text{--}40$ keV range. Since QPOs and coherent pulsations are usually stronger at these energies (e.g. Morgan, Remillard & Greiner 1997; Rodriguez et al. 2004, 2006b), this ensures a higher sensitivity to any feature that might exist. We produced power density spectra (PDS) from each of the individual light curves between ~ 0.02 and 4096 Hz.

2.2. Radio observations

IGR J17497–2821 was observed on Sept. 26 and 27, 2006, with the ATCA, located at Narrabri, Australia. The array was in the H75 configuration (allowing a baseline as long as 6 km) with antennas 1 and 5 off-line due to maintenance. Observations were carried out simultaneously at 4.80 GHz (6 cm) and 8.64 GHz (3.5 cm), with a continuum bandwidth of 128 MHz, for a total of about 12.3 hours on source. The amplitude and band-pass calibrator was PKS 1934–638, and the antennas’ gain and phase calibration, as well as the polarization leakage, were derived from regular observations of the nearby calibrator TXS 1748–253. The editing, calibration, Fourier transformation, deconvolution, and image analysis were performed using the MIRIAD software package (Sault & Killen 1998). No radio emission from IGR J17497–2821 was detected with ATCA on either date. Combining the two sets of observations resulted in the three sigma upper limits for IGR J17497–2821 of 0.21 mJy at both frequencies.

3. RESULTS OF THE X-RAY ANALYSIS

Fig. 1 shows the light curves seen by Swift/BAT and *RXTE*/PCA. In about 5 days the 15-50 keV BAT flux increased by a factor greater than 5, and remained around 0.02 cts/s until MJD 54006. The BAT flux is not purely

constant though, since it showed the presence of two peaks. After MJD 54006 a significant decrease is seen (Fig. 1). From the quality of the data, it is difficult to say whether the shape of the BAT light curve is FRED-like, or if the decay is purely linear. In fact, fitting the decay with an exponential leads to an e-folding time of 16.9 days.

The spectra were first fitted with a simple absorbed power law model. In all cases, the power law photon index was hard (~ 1.56). Although the reduced χ^2 was relatively acceptable (1.5 for 96 degrees of freedom (DOF) for Obs. 1), a slight deviation was visible at high energy. Adding a cutoff improved the fit. An F-test yielded a probability of 2.8×10^{-3} that the improvement was purely due to chance. In all observations except 4, 5 and 6 the cutoff was required at a high level of significance. This may indicate that it was either truly absent in obs. 4, 5 and 6, or that the cutoff energy had increased closer to the upper boundary of our spectral analysis. Note that these three observations occur between the two peaks of the BAT light curve (Fig. 1).

Since a hard power law with an exponential cutoff is usually interpreted in XRBs as being due to thermal Comptonization, the pure phenomenological model was replaced by the `comptt` model (Titarchuk 1994). The same model was applied to all observations to ease the comparison. In all cases, a hint for an iron edge at ~ 7 keV was visible. Adding such a feature greatly improved the fits (1.7×10^{-9} chance improvement). The mention by Itoh et al. (2006) of such a feature in the *Suzaku* spectrum of the source lent further credibility to this detection. The optical depth of the Edge ranges from 0.08 to 0.12, while the reduced χ^2 ranges from 0.97 to 1.14 for 93 DOF. All other fit parameters are reported in Table 2, while Fig. 2 shows the spectrum from Obs. 7. The source spectral parameters were relatively stable over the period of observations. Slight differences are found only for Obs. 1 & 7, for which the electron temperatures seem higher, although poorly constrained.

The 1-s bin PCA light curves extracted from the 7 observations showed no particular differences. No obvious dips, eclipses, or X-ray bursts were visible¹⁰. To quantify the degree of variability, we inspected each PDS individually. The variability of IGR J17497–2821 is dominated by frequencies lower than 1 Hz (Fig. 3 for Obs. 1). We modeled the PDSs with the help of broad Lorentzians (Belloni et al 2002a). As in typical PDSs of XRBs, three such features are needed (van der Klis 2006), two with their centroid frozen to 0 and one representing the so called low frequency hump (LFH). Broad Lorentzians mimic a flat top component and power law decay above a break frequency. The analogue of the break frequency is given by $\Delta = \sqrt{(\sigma/2)^2 + \nu_0^2}$, with σ the full width at half maximum, and ν_0 the centroid frequency (Belloni et al 2002a). The PDSs from the different observations showed very little variations. The 3 components were compatible (within the errors) with being constant through the outburst. As a reference the parameters we obtained for Obs. 1 are $\Delta = 0.06 \pm 0.01$ Hz, $\text{RMS} \sim 13 \pm 2\%$, for the main component $\Delta = 1.8 \pm 0.7$ Hz, $\text{RMS} = 10 \pm 2\%$ for the second, and $\nu_0 = 0.30 \pm 0.07$ Hz, $\Delta = 0.23 \pm 0.07$ Hz, $\text{RMS} = 13 \pm 2\%$ for

¹⁰In the PCU 3 light curve of Obs. 2, however a large flare was detected. This was not confirmed while inspecting all other active PCUs. This flare seems to be purely instrumental.

the LFH. The total RMS variability is then $\sim 36\%$ RMS. The 3σ upper limit for a 2 Hz FWHM QPO is 2%.

We searched for X-ray pulsations between ~ 0.2 ms and 256 s in the unbinned PDSs. We do not detect any coherent pulsations in any of them. While below 1 Hz the significant level of aperiodic noise renders our search less sensitive to the detection of a given feature, above 1 Hz a periodic signal would be more readily detectable out of the white noise. From the PDS of Obs. 1, and with a frequency resolution of 3.9×10^{-3} Hz, we could calculate 3σ upper limits of 0.9% between 1 and 4096 Hz. Below 1 Hz, using a similar approach (assuming here that a pulsation should appear out of the level of aperiodic noise, and using the “flat top” level below 0.3 Hz), we could calculate that the limit for a coherent pulsation ranges from $\sim 2.4\%$ at 0.4 mHz to $\sim 1\%$ at 1 Hz.

4. DISCUSSION

We analyzed a set of *RXTE* observations of the newly-discovered source IGR J17497–2821. The PDSs of IGR J17497–2821 are typical of XRBs in the LHS (e.g. van der Klis 2006). Although the general shape of the PDSs makes it difficult to discriminate a NS from a BH (van der Klis 2006), the typical frequencies are believed to be lower in the case of BH (the ms accreting pulsar IGR J00291+5934 being a recent counter example). In fact Sunyaev & Revnivtsev (2000) observed that in the LHS for BH systems no significant signal is detected above ~ 50 Hz, contrary to weakly magnetized NS. In IGR J17497–2821 the lack of significant signal above ~ 10 Hz, above which the level of variability is compatible with being purely due to Poisson noise, and the high level of the flat top noise together with the low frequency of the break in the first Lorentzian component (0.06 Hz) are reminiscent of BH systems. Generally speaking, and although this is not a proof, none of the characteristics that would make IGR J17497–2821 a definite NS (kHz QPOs, X-ray bursts, coherent pulsations) are observed.

The source spectrum is well represented by a power law (with $\Gamma \sim 1.57$) convolved by interstellar absorption and a high-energy cutoff starting at $E_{\text{cut}} \sim 50$ keV with a folding energy $E_{\text{fold}} \sim 190$ keV, which are all typical of XRBs in the LHS. This is usually interpreted as due to thermal Comptonization of soft X-ray photons on a population of energetic electrons. Whether these electrons form a “corona” or the base of a compact jet is subject to debate (e.g. Markoff et al. 2005). A thermal Comptonization model represents the spectra well. The high value of the electron temperature and the optical depth, suggest that the compact object probably a BH. Indeed, with $E_{\text{cut}} = 3 \times kT_e$, we obtain an equivalent cutoff energy of about 100-120 keV which is similar to e.g. Cyg X-1 while in the LHS (Cadolle Bel et al. 2006b), or XTE J1550–564 during its 2002 outburst (Belloni et al 2002b)), two well known BHs. In addition, even if some extremely hard NS Atoll sources can show similar spectra, the values of τ obtained in those cases are systematically higher (Barret 2001) than those of IGR J17497–2821.

The (unabsorbed) 1-20 and 20-200 keV luminosities are $1.1 \times 10^{37} \times (d/8kpc)^2 \text{erg/s}$ and $2.1 \times 10^{37} \times (d/8kpc)^2 \text{erg/s}$.

At the distance of the Galactic Center, these luminosities place the source outside the so-called burster box (Barret et al. 2000), in fact very close to Cyg X-1 in its LHS. Although several NS sources have been seen to lie outside this box, they all have their 20–200 keV luminosity lower than $\sim 10^{37} \times \text{erg/s}$. In this respect, if IGR J17497–2821 is located at a large distance, as possibly suggested by the high value of the equivalent absorption column density, its hard luminosity strongly suggests that it contains a BH.

Fig. 4 shows the position of IGR J17497–2821 w.r.t. the radio-X-ray correlation. IGR J17497–2821 lies below the expected correlation for BHs. Fig 4 (see Corbel et al. 2004; Cadolle Bel et al. 2006a) shows that some BH(C)s have been observed to lie below the expected correlation. The non-detection of IGR J17497–2821 in radio is therefore not an argument against a BH primary. Given the results of our X-ray spectral analysis, we conclude that IGR J17497–2821 is a BHC in its LHS. The observations of sources for which the correlation between the radio and X-ray fluxes is not observed suggest that, contrary to other BHs in the LHS, the formation and/or emission from the jet may be prevented for some unknown reasons.

Recently several sources have been observed to remain in the LHS during the whole duration of their outburst. These sources can either host a NS (e.g. Aql X-1), or a BH(C) (XTE J1550–564, Swift J1753.5–0127, GRO J0422+32, GRO J1719-24, and XTE J1118+480; Sturmer & Shrader (2005); Cadolle Bel et al. (2006a); Brocksopp et al. (2004)). Interestingly Aql X-1 and XTE J1550–564 are also known to undergo major outbursts. The existence of LHS outbursts in XRBs brings interesting questions regarding the physics of accretion. In XTE J1550–564, Sturmer & Shrader (2005) have suggested that this outburst could correspond to a discrete accretion event. Rodriguez et al. (2006a) have suggested the same could also occur in Aql X-1. In both these cases, the outbursts had a short duration (~ 30 -40 days) compared to their previous outbursts. The similar duration of the outburst of IGR J17497–2821 could by comparison indicate that a similar event took place. As pointed out by Sturmer & Shrader (2005) the LHS outburst in GRO J0422+32, GRO J1719-24, and XTE J1118+480 could (by opposition to at least XTE J1550–564) be explained by a lower reservoir of material, these sources having a short orbital periods. Although we cannot know whether IGR J17497-2821 will have a major outburst in the future, the fact that the companion of IGR J17497–2821 is a red giant K-type star (Paizis et al. 2006) rules out a system with such a short orbital period.

We are especially grateful to J. H. Swank and the *RXTE* mission planners for having accepted our ToO, and for their very rapid reaction to plan our observations. The Swift/BAT transient monitor results are kindly provided by the Swift/BAT team. J.R. would like to thank S. Chaty for useful discussions. This research has made use of data obtained through the High Energy Astrophysics Science Archive Center Online Service, provided by the NASA/Goddard Space Flight Center.

REFERENCES

- Barret, D. 2001, *Adv. Space Res*, 28, 307
 Barret, D., Olive, J.-F., Boirin, L., et al. 2000, *ApJ*, 533, 329
 Belloni, T., Psaltis, D., van der Klis, M. 2002a, *ApJ*, 72, 392
 Belloni, T., Colombo, A.P., Homan, J., Campana, S., van der Klis, M. 2002b, *A&A*, 390, 199
 Brocksopp, C., Bandyopadhyay, R.M., Fender, R.P. 2004, *NewA.*, 9, 249
 Cadolle Bel, M., Ribó, M., Rodriguez, J., et al., 2006a, submitted to *ApJ*
 Cadolle Bel, M., et al. 2006b, *A&A*, 446, 591
 Corbel, S., Nowak, M. A., Fender, R. P., Tzioumis, A. K., & Markoff, S. 2003, *A&A*, 400, 1007
 Corbel, S., Fender, R.P., Tomsick, J.A, et al. 2004, *ApJ*, 617, 1272
 Dickey, J.M. & Lockman, F.J. 1990, *ARA&A*, 28, 215
 Gallo, E., Fender, R.P., Pooley, G.G. 2003, *MNRAS*, 344, 60
 Hynes, R. I., Mauche, C. W., Haswell, C. A., Shrader, C. R., Cui, W., & Chaty, S. 2000, *ApJ*, 539, L37
 Itoh, T., Kokubun, M., Yuasa, T., et al. 2006 *ATel* 914
 van der Klis 2006, in *Compact Stellar X-ray sources*, Eds. Lewin & van der Klis, Cambridge University Press
 Kuulkeers, E., Chenevez, J., Shaw, S., et al. 2006, *ATel* 888
 Maccarone, T.J. 2003, *A&A*, 409, 697
 Markoff, S., Nowak, M. A., & Wilms, J. 2005, *ApJ*, 635, 1203
 Markwardt, C.B. & Swank, J.H. 2006 *ATel* 891
 Migliari, S. & Fender, R.P. 2006, *MNRAS*, 366, 79
 Morgan, E.H., Remillard, R.A & Greiner, J. 1997, *ApJ*, 482, 993
 Paizis, A., Nowak, M., Chaty, S., Rodriguez, J., Courvoisier, T. J.-L. et al. 2006, submitted to *ApJ*, astro-ph 0611344
 Rodriguez, J., Corbel, S. & Tomsick, J.A. 2003, *ApJ*, 595, 1032
 Rodriguez, J., Corbel, Hannikainen, D.C., Belloni, T. Paizis, A. & Vilhu, O. 2004, *ApJ*, 615, 416
 Rodriguez, J., Shaw, S.E. & Corbel, S. 2006a, *A&A*, 451, 1045
 Rodriguez, J., Bodaghee, A., Kaaret, P., et al. 2006b, *MNRAS*, 366, 274
 Soldi, S., Walter, R., Eckert, D., et al. 2006, *ATel* 885
 Sturmer, S.J., Schrader, C.R. 2005, *ApJ*, 625, 923
 Sunyaev, R. & Revnivtsev, M. 2000 *A&A*, 358, 617
 Titarchuk, L. 1994, *ApJ*, 434, 313

TABLE 1

JOURNAL OF THE *RXTE* OBSERVATIONS ANALYZED IN THIS PAPER. MJD 54000 IS SEPT. 22., 2006 THE LAST TWO COLUMNS INDICATE THE NET COUNT RATES FROM PCA/PCU2 (3-30 KEV) AND HEXTE/CLUSTERB (18-200 KEV).

| Obs. # | Obs. Id (P92016) | MJD (d) | GTI (s) | Count rates | |
|--------|------------------|---------|---------|-------------|-------|
| | | | | PCA | HEXTE |
| 1 | 01-01-00 | 53998.2 | 6384 | 61.4 | 13.3 |
| 2 | 01-02-00 | 54000.2 | 3200 | 67.5 | 14.5 |
| 3 | 01-01-02 | 54001.3 | 3200 | 68.4 | 14.3 |
| 4 | 01-02-01 | 54002.0 | 2368 | 66.7 | 14.3 |
| 5 | 01-02-02 | 54003.2 | 3216 | 64.5 | 15.3 |
| 6 | 01-01-01 | 54005.0 | 3232 | 60.8 | 13.0 |
| 7 | 01-03-00 | 54007.1 | 6480 | 53.8 | 12.2 |

TABLE 2

BEST FIT PARAMETERS OBTAINED FROM THE COMBINED PCA+HEXTE SPECTRA. THE SPECTRAL MODEL CONSISTS OF **phabs*edge*comptt**. IN ALL CASES THE REDUCED χ^2 IS AROUND 1. THE SEED PHOTON TEMPERATURE FOR COMPTONIZATION WAS FROZEN TO 0.1 KEV IN ALL CASES. ERRORS ARE GIVEN AT THE 90% CONFIDENCE LEVEL. $\dagger \times 10^{22} \text{ cm}^{-2}$. *3-20 KEV UNABSORBED $\times 10^{-9} \text{ ERG CM}^{-2} \text{ S}^{-1}$.

| Obs. # | N_{H}^{\dagger} | Edge keV | kT_e keV | τ | flux* |
|--------|--------------------------|---------------------|-------------------|---------------------|-------|
| 1 | 4.1 ± 0.4 | 6.8 ± 0.3 | 37_{-7}^{+118} | $1.6_{-1.0}^{+0.3}$ | 1.0 |
| 2 | 3.8 ± 0.4 | 6.6 ± 0.3 | 34_{-6}^{+21} | $1.8_{-0.6}^{+0.3}$ | 1.14 |
| 3 | 3.9 ± 0.4 | 6.7 ± 0.3 | 33_{-5}^{+12} | $1.8_{-0.4}^{+0.2}$ | 1.16 |
| 4 | 3.8 ± 0.5 | $7.1_{-0.3}^{+0.4}$ | 33_{-5}^{+16} | $1.9_{-0.5}^{+0.3}$ | 1.13 |
| 5 | 3.3 ± 0.4 | $6.8_{-0.3}^{+0.4}$ | 37_{-6}^{+25} | $1.7_{-0.5}^{+0.3}$ | 1.08 |
| 6 | 3.5 ± 0.4 | $6.8_{-0.3}^{+0.4}$ | 40_{-8}^{+22} | $1.7_{-0.5}^{+0.3}$ | 1.02 |
| 7 | 3.6 ± 0.4 | 6.8 ± 0.3 | $38_{-7}^{+88.0}$ | $1.7_{-1.1}^{+0.3}$ | 0.91 |

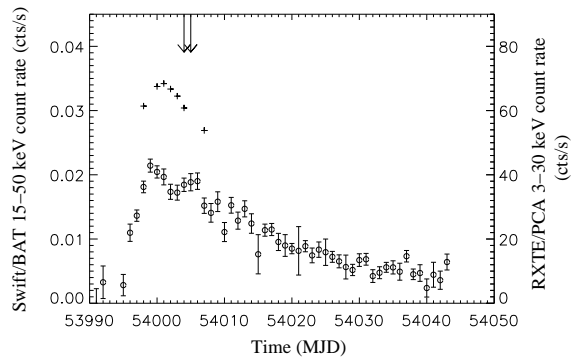


FIG. 1.— 15–50 keV Swift/BAT (open circles) and 3–30 keV *RXTE*/PCA (crosses) light curves of IGR J17497–2821 during the outburst studied in this paper. The vertical arrows represent the dates of our ATCA observations. For BAT 1 Crab ~ 0.23 cts/s and ~ 1840 cts/s for PCA.

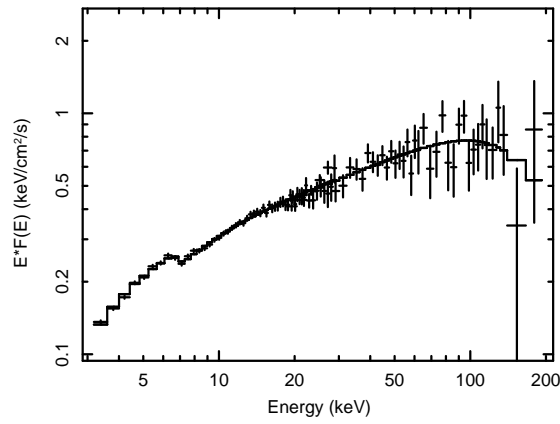


FIG. 2.— 3–200 keV *RXTE* spectrum of Obs. 7. The best model is superimposed as a line.

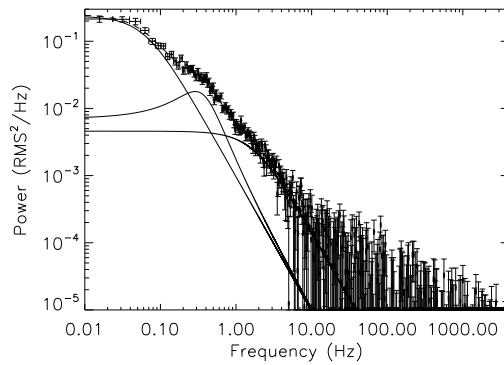


FIG. 3.— White noise corrected PDS from Obs. 1. The continuous lines represents the 3 broad Lorentzians used to model the PDS. The dashed lines is the best model.

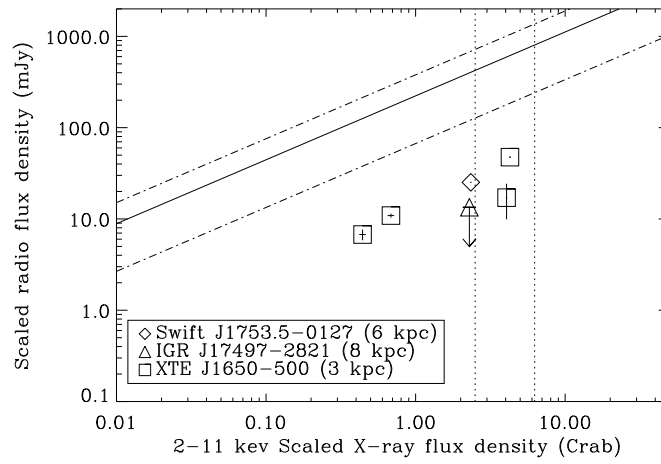


FIG. 4.— Plot of the radio vs. X-ray fluxes for the BH XTE J1650–500 (Corbel et al. 2004), the BHC Swift J1753.5–0127 (Cadolle Bel et al. 2006a), and IGR J17497–2821 with their (assumed) distances. All fluxes are normalized to a distance of 1 kpc. The range of correlated radio/X-ray fluxes is indicated by the dashed dot lines, while the continuous line indicates the best position. The vertical dotted lines indicate 2% and 5% of the Eddington luminosity.